Research Square

Preprints are preliminary reports that have not undergone peer review.
They should not be considered conclusive, used to inform clinical practice,
or referenced by the media as validated information.

The Natural Alkaloid Bousigonine D Improves Insulin Sensitivity and Glucose Homeostasis through Concurrent PI3K/AKT and AMPK Activation

Hedi Wang
Shandong University of Traditional Chinese Medicine
Qiang Chen
Shandong University of Traditional Chinese Medicine
Qianhui Ning
Shandong University of Traditional Chinese Medicine
Zhiwei Wang
Shandong First Medical University
Yanting Lu
luyanting922@163.com
Shandong University of Traditional Chinese Medicine

Research Article

Keywords: Monoterpenoid indole alkaloids;Type 2 diabetes mellitus；Insulin resistance；PI3K, AKT, AMPK pathway；Bousigonia mekongensis；Glucose metabolism；Insulin sensitivity

Posted Date: November 16th, 2026

DOI: https://doi.org/10.21203/rs.3.rs-11243720/v1

License: This work is licensed under a Creative Commons Attribution 4.0 International License.
Read Full License

Additional Declarations: No competing interests reported.

The Natural Alkaloid Bousigonine D Improves Insulin Sensitivity and Glucose Homeostasis through Concurrent PI3K/AKT and AMPK Activation

Hedi Wang[1], Qiang Chen[1], Qianhui Ning[1], Zhiwei Wang[4*], Yanting Lu[2,3*]

[1] College of Traditional Chinese Medicine, Shandong University of Traditional Chinese Medicine, Jinan, Shandong, People's Republic of China; [2] Shandong Co-Innovation Center of Classic TCM Formula, Shandong University of Traditional Chinese Medicine, Jinan, Shandong, People's Republic of China; [3] School of Medicine, Shandong University of Traditional Chinese Medicine, Jinan, 250014,Shandong, People's Republic of China; [4] School of Pharmaceutical Sciences & Institute of Materia Medica, Shandong First Medical University & Shandong Academy of Medical Sciences, National Key Laboratory of Advanced Drug Delivery System, Jinan 250117, Shandong, China

*Corresponding author. College of Medicine, Shandong University of Traditional Chinese Medicine,Jinan,250355, Shandong,China. (Y.-T.Lu) ;School of Pharmaceutical Sciences & Institute of Materia Medica, Shandong First Medical University & Shandong Academy of Medical Sciences, National Key Laboratory of Advanced Drug Delivery System, Jinan 250117, Shandong, China. (Z.-W. Wang)

E-mail address: luyanting922@163.com (Y.-T.Lu) ; wzwcpu@126.com (Z.-W. Wang)

Abstract

Type 2 diabetes mellitus (T2DM) is a chronic metabolic disorder driven primarily by insulin resistance and disordered glucose and lipid metabolism, which poses a substantial global health and economic burden. This study was designed to evaluate the therapeutic potential of Bousigonine D (BSG-D), a monoterpenoid indole alkaloid from Bousigonia mekongensis, and to elucidate its underlying mechanisms in ameliorating insulin resistance and associated metabolic dysregulation in T2DM. Using a combination of in vivo (high-fat diet plus streptozotocin-induced diabetic mouse model) and in vitro (HepG2 insulin-resistant cell model) experimental approaches, along with biochemical assays, histopathological examination, and analysis of protein expression, we found that administration of BSG-D induced a rapid reduction in blood glucose levels within 6 hours in diabetic mice and improved systemic glucose homeostasis, as demonstrated by enhanced performance in both oral glucose tolerance and insulin tolerance tests. BSG-D treatment also effectively modulated serum lipid profiles, lowering total cholesterol and free fatty acids levels. Histopathological examination revealed that BSG-D ameliorated pancreatic and hepatic damage, characterized by improved cellular architecture and diminished inflammatory infiltration. Consistent with these effects in vivo, as shown by decreased serum insulin levels and a reduced HOMA-IR index, BSG-D restored glucose consumption in insulin-resistant HepG2 cells. These findings highlight the multifaceted therapeutic potential of BSG-D in T2DM management, supporting its promise as a novel therapeutic agent. Future studies should prioritize clinical validation and incorporate multi-omics strategies to further elucidate the mechanisms of action of BSG-D and advance its application in T2DM treatment.

Keywords: Monoterpenoid indole alkaloids ;Type 2 diabetes mellitus ;Insulin resistance ; PI3K/AKT/AMPK pathway ; Bousigonia mekongensis ; Glucose metabolism ; Insulin sensitivity

Introduction

Type 2 diabetes mellitus (T2DM) has emerged as a major global health issue, accounting for nearly 90% of the approximately 537 million diabetes cases worldwide [1]. Its prevalence is rising alarmingly, particularly among children and young adults [2], largely due to adverse lifestyle changes [3]. The disease compromises quality of life and imposes a considerable socioeconomic burden due to increased healthcare costs and reduced productivity [4]. However, current major treatments are often hindered by limited efficacy, side effects, and poor adherence [5] . This therapeutic inadequacy has thus spurred the search for novel agents, especially natural products known for their multi-targeted activities and historical use in traditional medicine [6].

Bousigonia mekongensis (Apocynaceae), traditionally used in Dai medicine in China and a key ingredient of the "Baijie" capsule [7], produces a spectrum of alkaloids with documented antitumor activity [8-11]. In diabetes research, particular interest has focused on the monoterpene indole alkaloid Bousigonine D (BSG-D), which has been reported to ameliorate podocyte injury, indicating potential renal protective effects against diabetic nephropathy [12]. However, its impact on the fundamental pathological features of Type 2 diabetes mellitus (T2DM), specifically systemic insulin resistance and glucose metabolic dysregulation, remains unexplored.

To address this gap, we isolated the principal alkaloid from the roots of B. mekongensis. Comprehensive spectroscopic analysis, including HRMS, 1D (^{1}H and ^{13}C) and 2D NMR (Supplementary Figure 1), unequivocally identified the isolated compound as the known alkaloid BSG-D by comparison with literature data [9]. Its confirmed chemical structure is presented in Figure 1. Notably, the crystalline form of BSG-D obtained in our study exhibited different solubility properties compared to prior reports, likely due to polymorphic differences. With the authenticated compound thus obtained, we

subsequently evaluated its effects on core metabolic dysfunctions associated with T2DM.

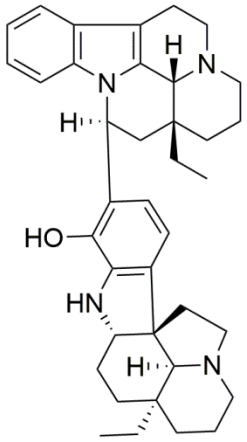


Figure 1. Chemical structure of the monoterpene indole alkaloid Bousigonine D (BSG-D) isolated from Bousigonia mekongensis.

A fundamental mechanism underlying IR involves the disruption of essential signaling pathways. The phosphoinositide 3-kinase/protein kinase B (PI3K/AKT) pathway serves as a primary mediator of insulin action [13-15], while the AMP-activated protein kinase (AMPK) pathway plays a central role in regulating cellular energy homeostasis [16-18]. Consequently, dysregulation of both PI3K/AKT and AMPK signaling pathways is critically involved in the pathogenesis of IR and T2DM [19-20]. Insulin binding initiates PI3K/AKT pathway activation, resulting in the generation of phosphatidylinositol (3,4,5)-trisphosphate (PIP3), phosphorylation of AKT, and subsequent regulation of downstream effectors that promote glycogen synthesis and suppress hepatic glucose production[21-23].Meanwhile, AMPK functions as a cellular energy sensor that enhances glucose uptake and fatty acid oxidation in peripheral tissues while suppressing hepatic gluconeogenesis, thereby improving insulin sensitivity [24-25]. Notably, AMPK and AKT exhibit cross-regulatory interactions. Under IR conditions, impaired AMPK activity exacerbates dysregulated glycemia and lipid metabolism, which further impairs insulin responsiveness [26-28]. Collectively, the interplay between the PI3K/AKT and AMPK pathways is essential for maintaining glucose homeostasis, and their dysfunction constitutes a critical mechanism in the pathogenesis of IR and T2DM.

In this study, we investigate the therapeutic potential of BSG-D in modulating glucose

and lipid metabolism in experimental T2DM, focusing on its action through the PI3K/AKT/AMPK signaling axis. An integrated strategy utilizing both in vivo and in vitro models was employed. A diabetic mouse model induced by high-fat diet and streptozotocin was established to recapitulate the systemic metabolic features of T2DM, while insulin-resistant HepG2 cells were used to elucidate cell-autonomous mechanisms. Together, our findings provide mechanistic insights and preclinical validation that support the development of BSG-D as a potential therapeutic candidate for T2DM.

Materials and Methods

1. Isolation and Purification of BSG-D.

The roots of *Bousigonia mekongensis* (18.0 kg) were powdered and extracted exhaustively with 95% ethanol under reflux. The combined ethanol extracts were concentrated under reduced pressure to afford a crude extract. This extract was suspended in water and acidified to pH 2–3 using 2% HCl, followed by extraction with dichloromethane (DCM). The aqueous phase was then basified to pH 9–10 with 10% NaOH and extracted with DCM to obtain the total alkaloid fraction (164.0 g). This fraction was subjected to silica gel column chromatography and eluted with a stepwise gradient of DCM/MeOH (from 40:1 to 1:1, v/v). Based on HPLC analysis, the eluates were pooled into eight fractions (Fr.C1–Fr.C8). A portion of Fr.C4 (2.0 g out of 16.7 g) was repeatedly recrystallized from methanol to afford a white precipitate (345 mg). HPLC-UV analysis showed that the purity of this compound was 95.3%.

2. Animals.

Forty specific pathogen-free (SPF)-grade male C57BL/6N mice were procured from Beijing Vital River Laboratory Animal Technology (Beijing, China). All animal experiments were conducted following the Guide for the Care and Use of Laboratory Animals and approved by the Institutional Animal Care and Use Committee of Shandong University of Traditional Chinese Medicine（SDUTCM20230307001）.

3. Model Establishment and Experimental Grouping.

In vivo: A total of forty mice were randomly divided into four groups (n=10/group): the

control group (Con), the type 2 diabetes model group (DM), and two DM groups treated with either a low or high dose of BSG-D (designated as BSG-D-L and BSG-D-H, respectively). The Con group was fed a standard diet, while the other three groups (DM, BSG-D-L, and BSG-D-H) were maintained on a high-fat diet for the entire study period. After four weeks, mice in the DM, BSG-D-L, and BSG-D-H groups were fasted for 12 h. Then, streptozotocin was administered intraperitoneally at 50 mg/kg daily for three consecutive days to induce type 2 diabetes.

In vitro: HepG2 cells were cultured until they reached 80%-90% confluence and then passaged. The cells were divided into five groups: control (Con), insulin resistance (IR), IR treated with BSG-D, IR treated with BSG-D plus the AKT inhibitor MK-2206, and IR treated with BSG-D plus the AMPK inhibitor Dorsomorphin. The Con group was maintained in normal DMEM medium. All other groups were serum-starved for 24 h and then stimulated with insulin (1×10^{-5} mol/L) to induce IR. During insulin stimulation, the BSG-D group received BSG-D compound, while the MK-2206 and Dorsomorphin groups were co-treated with BSG-D and the respective inhibitor. All cells were incubated at 37°C for 48 h prior to analysis.

4. Measurement of Mouse Blood Glucose.

Random blood glucose (RBG) levels were measured daily at a consistent time point via tail vein blood collection from non-fasted mice. To evaluate the acute glucose-lowering effect, Post-treatment Blood Glucose (PTBG) levels were measured within 6 h after drug administration. For comprehensive metabolic characterization, oral glucose tolerance test (OGTT) and insulin tolerance test (ITT) were performed. Blood glucose was measured at 0, 30, 60, and 120 minutes after glucose or insulin injection. The area under the curve (AUC) was calculated to quantify overall glycemic response.

5. Specimen Collection and Processing.

Mice were fasted for 12 h with free access to water. After anesthetizing the mice with isoflurane, blood samples were collected from the retro-orbital sinus. Blood was allowed to clot at room temperature for 30 minutes and then centrifuged at 4°C for 15 minutes at 3,000 rpm to obtain serum. Following blood collection, mice were euthanized by cervical

dislocation. The pancreas and liver were rapidly excised, rinsed with ice-cold PBS, and gently blotted dry. Pancreatic tissues and one liver lobe were fixed in 4% paraformaldehyde for 24 h, while the remaining tissues were snap-frozen and stored at -80℃ for further analysis.

6. ELISA Kit Detection of Mouse insulin and Calculation of HOMA-IR

Serum samples were prepared as previously described in Section 5. Insulin levels were measured using a commercial enzyme-linked immunosorbent assay (ELISA) kit (Elabscience Biotechnology Co., Ltd., Wuhan, China) according to the manufacturer's instructions. Briefly, serum samples were added to the pre-coated plate and incubated at 37℃ for 90 minutes. After aspiration of the liquid, biotinylated detection antibody working solution was added to each well and incubated for 1 h at 37℃. The plate was then washed three times with wash buffer. Horseradish peroxidase conjugate working solution was added and incubated for 30 minutes at 37℃, followed by washing five times. The substrate reagent was then added and incubated for 15 minutes at 37℃ in the dark. The reaction was terminated with the stop solution, and the absorbance was immediately measured at 450 nm using a microplate reader (BioTek Instruments, Inc., Winooski, VT, USA). A standard curve was generated using known concentrations of insulin provided by the kit, and serum insulin concentrations were calculated accordingly. The homeostasis model assessment of insulin resistance (HOMA-IR) was calculated using the formula: HOMA-IR = fasting blood glucose × fasting insulin / 22.5.

7. Measurement of TG, TC, and FFA

Serum samples were prepared following the procedure detailed in Section 5. The concentrations of triglyceride (TG), total cholesterol (TC), and free fatty acids (FFA) in the serum were measured using commercial enzymatic assay kits (Jiancheng Bioengineering Institute, Nanjing, China), in accordance with the manufacturer's instructions. Briefly, reagents were prepared for blank, standard, and sample wells as specified in the kit protocols. Each sample was mixed with the corresponding working solution and incubated at 37℃. Absorbance was then measured for each well using a microplate reader (BioTek Instruments, Inc., Winooski, VT, USA) at 500 nm (TC, TG)

and 546 nm (FFA). Based on the standard curves, the concentrations of TG, TC, and FFA were calculated accordingly.

8. HE Staining of Liver Tissue.

Formaldehyde-fixed liver tissues were embedded in paraffin and sectioned for pathological analysis. After deparaffinization, the sections were stained with hematoxylin and eosin (HE). Then they were dehydrated, cleared, and mounted with neutral balsam. The stained sections were observed under an optical microscope (KEYENCE, Osaka, Japan) and images were captured and archived.

9. Measurement of Glucose Consumption.

After modeling and drug treatment, cells were cultured in normal medium for a set period. The supernatant was then collected, and glucose concentration was measured using a commercial glucose assay kit (Jiancheng Bioengineering Institute, Nanjing, China). A 2.5 μL aliquot of the cell culture supernatant was transferred to a 96-well plate, and 250 μL of working reagent was added. After incubation at 37°C for 10 minutes, the absorbance was measured at a wavelength of 505 nm. The glucose concentration was then calculated according to the formula provided by the manufacturer's instructions.

10.CCK-8 Assay for Cell Viability.

After modeling and drug treatment, 10 μL of the CCK-8 reagent (Ape×Bio Technology, Shanghai, China) was added to each well and the plate was incubated at 37℃ for 60 minutes in the dark. The optical density (OD) at 450 nm was then measured using a microplate reader (BioTek Instruments, Inc., Winooski, VT, USA), and cell survival rates were calculated accordingly.

11.Western Blot Analysis of Protein Expression in Liver Tissue and HepG2 cells.

Tissue samples from each group of mice and HepG2 cells were lysed in RIPA Lysis Buffer (Seven Innovation Biological Technology Co., Ltd., Beijing, China). The lysates were then centrifuged at 10,000 rpm for 10 minutes to collect the supernatant. Protein concentration was determined using a BCA protein assay kit (Boster Biological

Technology Co., Ltd., Wuhan, China). Subsequently, the samples were mixed with protein loading buffer, denatured by heating in a metal bath, and then stored at -20℃ for future use. Proteins were separated by SDS-PAGE according to their molecular weights. After electrophoresis, the separated proteins were transferred to PVDF membranes (Merck KGaA, Darmstadt, Germany). The membranes were then blocked with 5% skim milk solution for 2 h at room temperature, followed by incubation with primary antibodies at 4℃ overnight. The primary antibodies used were as follows: anti-AMPK, anti-phospho-AMPK(Thr172), anti-Akt, and anti-phospho-Akt（Ser450） (Cell Signaling Technology, Danvers, MA, USA); anti-actin (Wuhan SanYing Biotechnology Co., Ltd., Wuhan, China). After primary antibody incubation, membranes were incubated with corresponding secondary antibodies at room temperature for 1 h. The membranes were washed three times with TBST, incubated with ECL substrate (Boster Biological Technology Co., Ltd., Wuhan, China), and then visualized by chemiluminescent detection on Chemiluminescence imaging system (Wuhan Servicebio Biotechnology Co., Ltd., Wuhan, China).The gray intensity value of each band was measured using ImageJ software.

12. Statistics

Data are expressed as mean ± SD. Assessment of statistical significance was performed with a two-tailed Student's *t*-test using GraphPad Prism (version 9). A p value of less than 0.05 was considered statistically significant.

Results

1. BSG-D Lowers Blood Glucose and Ameliorates Insulin Resistance in Diabetic Mice.

To assess the hypoglycemic activity of BSG-D, blood glucose levels were determined following treatment. As shown in Figure 2A and B, administration of BSG-D resulted in marked reductions in blood glucose at multiple time intervals in diabetic mice compared with the model control group. Diabetic mice exhibited sustained hyperglycemia throughout the observation period (Figure 2C, D). In contrast, BSG-D-treated animals demonstrated consistently lower glucose levels. To evaluate the effects of BSG-D on

insulin resistance, OGTT and ITT tests were performed. Diabetic mice displayed impaired glucose tolerance and reduced insulin sensitivity relative to control mice. However, in BSG-D-treated diabetic mice, both glucose excursion during OGTT (except at the low dose) and the response in ITT were significantly improved (Figure 2E–H), indicating enhanced systemic insulin sensitivity.

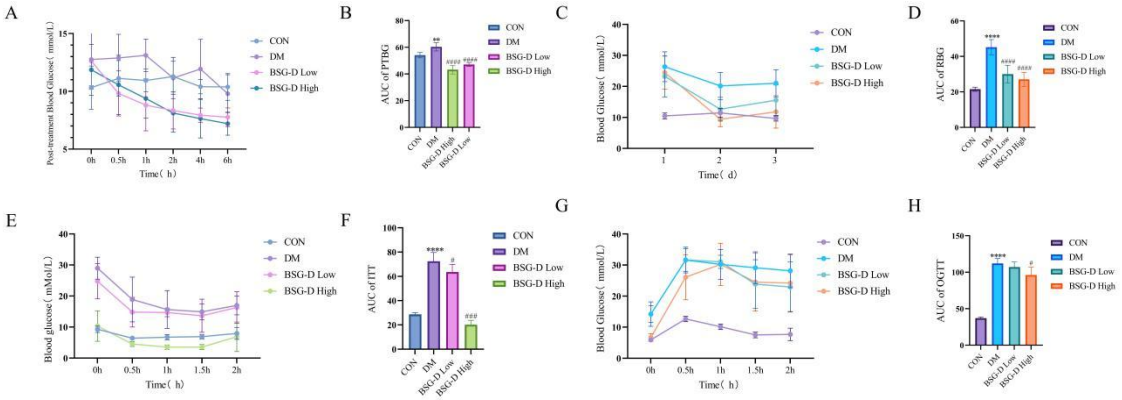


Figure 2. BSG-D improves glycemic control and insulin sensitivity in diabetic mice. (A) Change in post-treatment blood glucose (PTBG) blood glucose levels following BSG-D administration. (B) AUC for PTBG. (C) Random blood glucose level on day 3 after administration. D: AUC of random blood glucose over 3-day period. (E) Insulin tolerance test. (F) AUC for the ITT. (G) Oral glucose tolerance test. (H) AUC for the OGTT. Data are presented as mean ± SD. *p<0.05, **p<0.01, ***p<0.001, ****p<0.0001 vs. Control group. ##p<0.01, ###p<0.001, ####p<0.0001 vs. Model group.

2. BSG-D Attenuates Hyperlipidemia by Reducing Serum FFA and TC Levels in Diabetic Mice.

The effects of BSG-D on serum lipid parameters are presented in Figure 3. Diabetic mice exhibited significantly elevated total cholesterol (TC), triglyceride (TG), and free fatty acid (FFA) levels compared to the control group. BSG-D treatment produced significant reductions in FFA and TC levels. Although a decreasing trend in TG levels was observed, the difference did not reach statistical significance.

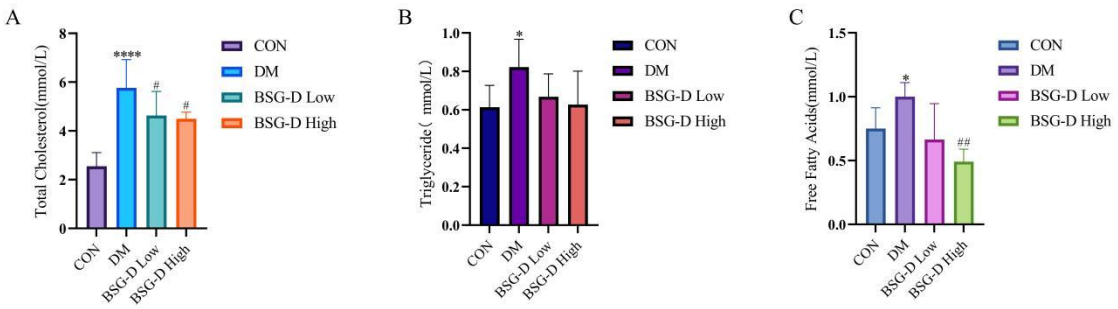


Figure 3. BSG-D ameliorates dyslipidemia in diabetic mice. (A) Serum total cholesterol (TC). (B) Serum triglyceride (TG) . (C) Serum free fatty acid (FFA). Data are presented as mean ± SD. *p<0.05, ****p<0.0001 vs. Control group. #p<0.05, ##p<0.01 vs. Model group.

3. BSG-D Attenuates Pancreatic and Hepatic Histopathological Injury in Diabetic Mice.

Histopathological analysis of pancreatic tissue by hematoxylin and eosin (H&E) staining revealed distinct morphological changes across groups. Control mice displayed normal pancreatic architecture with orderly arranged cells, intact morphology, and abundant cytoplasm. In contrast, pancreatic sections from diabetic mice exhibited severe structural disorganization, including loss of architectural integrity, blurred cellular boundaries, cytoplasmic reduction, vascular dilation, and signs of ductal proliferation, resulting in an overall reduction in pancreatic area. Treatment with BSG-D ameliorated these diabetic injuries, leading to a notable restoration of tissue integrity (Figure 4A, B).

Similarly, histological analysis of liver sections demonstrated neatly arranged hepatocytes in control animals. Diabetic mice, however, showed marked hepatic injury, characterized by cytoplasmic vacuolation, nuclear pyknosis, disorganized tissue structure, and inflammatory cell infiltration. Administration of BSG-D markedly attenuated these diabetic-induced pathological alterations, contributing to a partial restoration of hepatic histoarchitecture (Figure 4C, D).

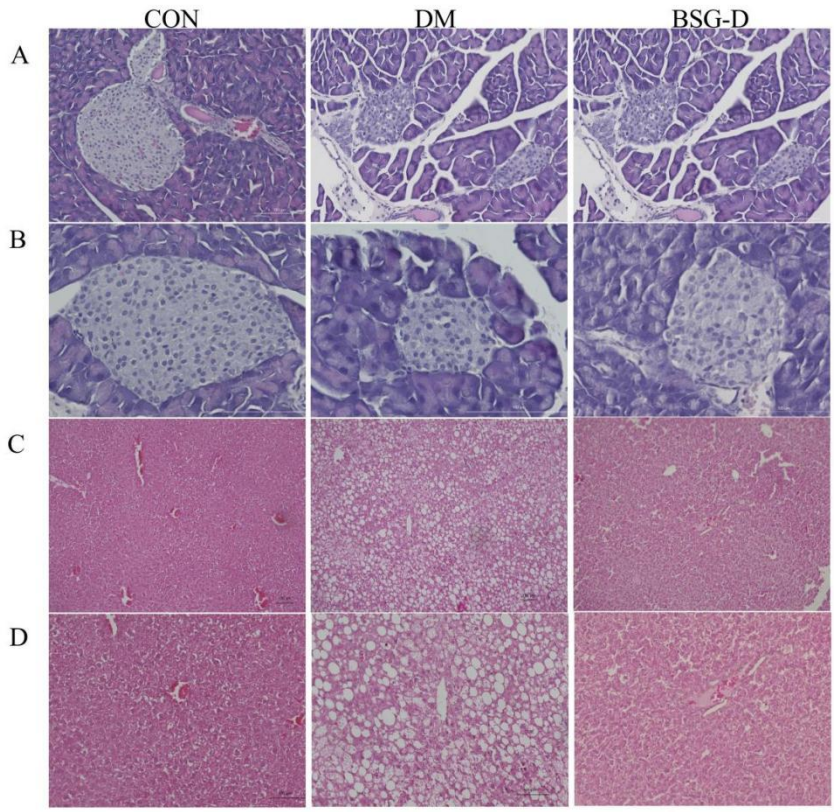


Figure 4. Histopathological assessment of pancreatic and hepatic tissues by H&E staining. (A) Pancreatic section (200x magnification). (B) Pancreatic section (400x magnification). (C) Hepatic section (200x magnification). (D) Hepatic section (400x magnification). Scale bar = 100μm (applies to all panels).

4. BSG-D Ameliorates Insulin Resistance *In Vitro* and *In Vivo*.

To investigate the effect of BSG-D on insulin resistance, this study combined both in vivo and in vitro approaches. Serum insulin levels and the HOMA-IR were evaluated in mice, while glucose consumption was assessed in insulin-resistant HepG2 cells. Diabetic mice exhibited significantly elevated insulin levels and HOMA-IR indices compared to control animals. BSG-D treatment markedly reduced both parameters, indicating improved systemic insulin sensitivity (Figure 5A, B). In vitro, insulin-resistant HepG2 cells exhibited significantly reduced glucose uptake compared to normal controls. Treatment with BSG-D enhanced glucose consumption in a dose-dependent manner, as confirmed in assays accounting for potential effects of cell viability (Figure 5C, D).

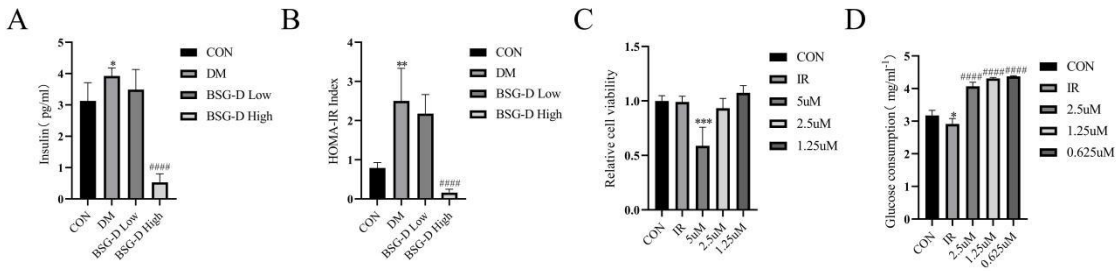


Figure 5. BSG-D improves insulin sensitivity *in vivo* and enhances glucose uptake *in vitro*. (A) Serum insulin levels. (B) Homeostasis model assessment of insulin resistance (HOMA-IR). (C) Viability of HepG2 cells treated with BSG-D. (D) Glucose uptake in insulin-resistant HepG2 cells. Data are presented as mean ± SD. *p<0.05, **p<0.01,***p<0.001 vs. Control group. ####p<0.0001 vs. Model group.

5. BSG-D Activates PI3K/AKT and AMPK Signaling in Diabetic Models.

To determine the effects of BSG-D on key insulin-sensitizing signaling pathways, we analyzed the protein expression of core signaling components. Western blotting was used to measure the levels of total and phosphorylated AKT and AMPK in mouse liver tissues (Figure 6A), and PI3K, AKT, and AMPK in insulin-resistant in HepG2 cells (Figure 6D). In both diabetic mice and cellular models, the phosphorylation states of these kinases were significantly suppressed. Treatment with BSG-D effectively restored the phosphorylation of AKT and AMPK in vivo and enhanced the phosphorylation of PI3K, AKT, and AMPK in vitro (Figure 6B-C, E-G), indicating a direct pharmacological action on these critical metabolic regulators.

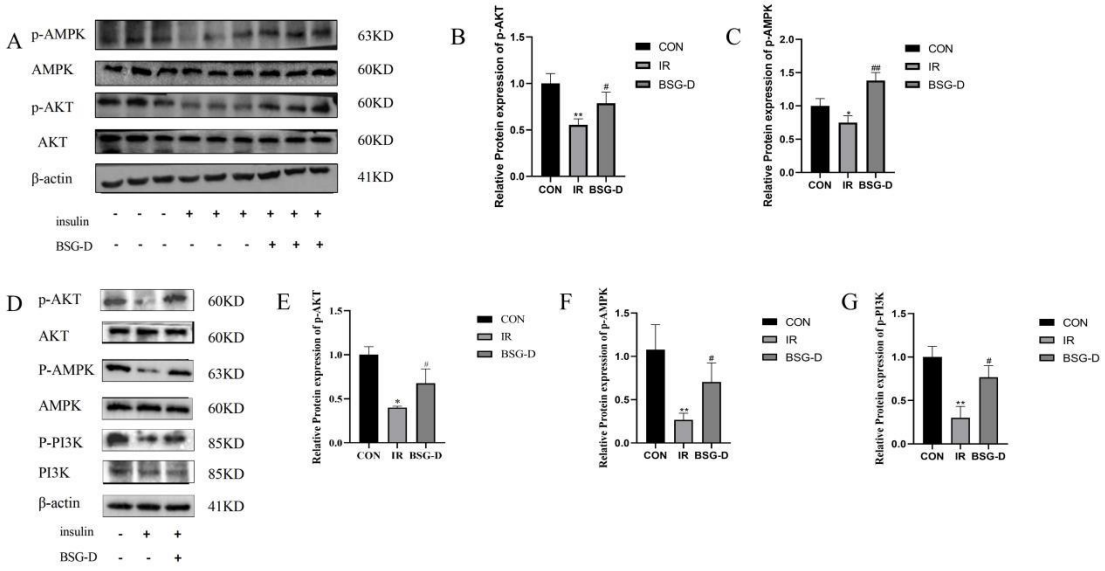


Figure 6. BSG-D activates PI3K/AKT and AMPK signaling in vivo and in vitro. (A) Representative immunoblots of AKT, p-AKT, AMPK, p-AMPK, and β-actin (loading control) in liver tissues from experimental mice. (B) Quantitative analysis of p-AKT/total AKT ratio. (C) Quantitative analysis of p-AMPK/total AMPK ratio. (D) Representative immunoblots of PI3K, p-PI3K, AKT, p-AKT, AMPK, p-AMPK, and β-tubulin (loading control) in insulin-resistant HepG2 cells. (E) Quantitative analysis of p-AKT/total AKT. (F) Quantitative analysis of p-AMPK/total AMPK. (G) Quantitative analysis of p-PI3K/total PI3K. Data are presented as mean ± SD. *p<0.05, **p<0.01 vs. Control group. #p<0.05, ##p<0.01 vs. Model group.

To establish the mechanistic link between the therapeutic effect of BSG-D and the PI3K/AKT/AMPK pathway, we employed pharmacological inhibition using Dorsomorphin (an AMPK inhibitor) and MK-2207 (an AKT inhibitor). Western blot analysis confirmed that both inhibitors significantly suppressed phosphorylation of their respective target proteins (Figure 7A). Subsequent glucose consumption assay revealed that pretreatment with either inhibitor markedly attenuated the enhancement of glucose uptake induced by BSG-D(Figure 7B). Potential confounding effects of cytotoxicity were excluded using CCK-8 viability assay (Figure 7C). These results demonstrated that both AMPK and AKT activation are necessary for BSG-D to ameliorate insulin resistance and enhance glucose utilization, indicating that the compound exerts its effects through simultaneous activation of these key signaling nodes.

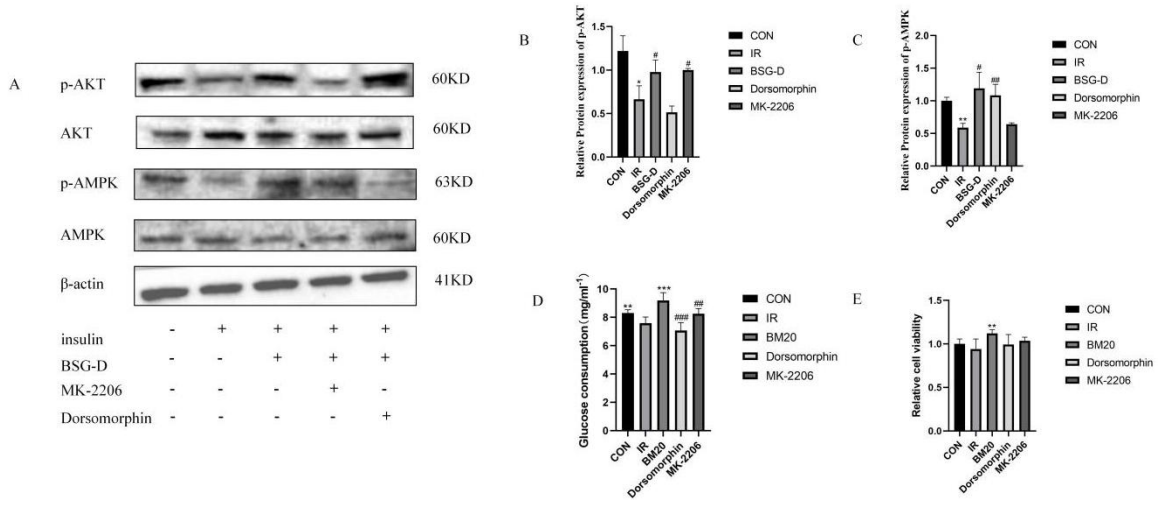


Figure 7. Pharmacological inhibition of AMPK and AKT attenuates BSG-D-induced glucose uptake. (A) Representative immunoblots of PI3K, p-PI3K, AKT, p-AKT, AMPK, p-AMPK, and β-tubulin (loading control) in HepG2 cells treated with BSG-D in the presence or absence of Dorsomorphin and MK-2206 . (B) Glucose uptake in insulin-resistant HepG2 cells following inhibition of AMPK/AKT signaling. C: Viability of HepG2 cells treated with inhibitor alone or in combination with BSG-D. Data are presented as mean ± SD. **p<0.01,***p<0.001 vs. Control group. ##p<0.01, ###p<0.001 vs. Model group.

Discussion

This study establishes that BSG-D, a monoterpenoid indole alkaloid isolated from *Bousigonia mekongensis*, elicits significant antihyperglycemic and insulin-sensitizing effects in a murine model of diabetes mellitus. Treatment with BSG-D produced rapid and dose-dependent reductions in random blood glucose, enhanced systemic glucose tolerance, and ameliorated diabetic dyslipidemia, as indicated by lowered serum total cholesterol and free fatty acid levels. Notably, BSG-D administration markedly attenuated pancreatic islet and hepatic histopathological injury and reduced the homeostasis model assessment of insulin resistance (HOMA-IR) index by more than 50%, demonstrating a robust improvement in overall insulin sensitivity.

Mechanistically, we demonstrate that the therapeutic benefits of BSG-D are mediated through the concurrent activation of the PI3K/AKT and AMPK signaling pathways. This conclusion is supported by the upregulation of phosphorylated AKT and AMPK in hepatic tissues and, critically, by the complete abolition of BSG-D-stimulated glucose uptake upon pharmacological inhibition of either AMPK or AKT. This dual-pathway activation is particularly significant, as it engages two fundamental and complementary

regulators of metabolism: the canonical insulin-signaling PI3K/AKT axis and the central cellular energy sensor AMPK. The synergistic action on these pathways likely underlies the compound's efficacy in improving both glycemic control and associated metabolic disturbances, positioning BSG-D as a promising candidate for further therapeutic development.

The efficacy profile of BSG-D observed across in vivo and in vitro models corroborates previously established mechanisms of certain MIAs. For example, its enhancement of insulin sensitivity and reduction in HOMA-IR reSDble the effects of serpentine, which augments insulin signaling through insulin receptor and AKT phosphorylation [29], as well as vindoline, which improves glycemic and lipid parameters in rodent models [30-32]. The restoration of glucose uptake in insulin-resistant HepG2 cells parallels that of akuammicine, an MIA reported to stimulate glucose uptake in adipocytes [33]. BSG-D may additionally share mechanistic features with other insulin-sensitizing MIAs that modulate protein tyrosine phosphatase 1B (PTP-1B) activity [34], though this hypothesis remains speculative and was not directly assessed in our study .

Notably, BSG-D exhibits a distinctive multifactorial efficacy profile. Whereas other MIAs—such as vindoline (primarily an insulin secretagogue) and serpentine (an insulin sensitizer)—demonstrate more specialized activities, BSG-D integrates direct insulin sensitization with pancreatic and hepatic protective effects. This broader pharmacological profile implies a multi-target mechanism of action, which may enable a more comprehensive therapeutic strategy against T2DM compared to single-pathway agents.

To fully delineate the therapeutic potential of BSG-D, further investigations should prioritize several key directions. First, precise identification of its direct molecular target(s) is essential. This includes evaluating potential interactions with signaling nodes such as PTP-1B or other phosphatases that fine-tune insulin receptor activity. Second, the glucoregulatory actions of BSG-D should be assessed in other insulin-responsive tissues—notably skeletal muscle and adipose tissue—to obtain a more integrated understanding of its systemic metabolic effects. Third, comprehensive toxicological profiling and long-term efficacy studies in relevant disease models are imperative to establish its safety and therapeutic durability, critical steps for translational advancement.

Finally, the multi-target mechanism of BSG-D furnishes a strong rationale for exploring its use in combination with existing antidiabetic agents. Such combinatorial strategies may produce synergistic efficacy, improve glycemic control, and potentially reduce side effects associated with high-dose monotherapies.

It is important to acknowledge the limitations of the present study. The current dataset lacks genomic or transcriptomic analyses, which precludes a multi-omics understanding of BSG-D's mechanism and potential effects on gene networks involved in insulin signaling or β-cell function. Furthermore, as with any preclinical studies, the translatability of these findings from murine and cellular models to human pathophysiology requires rigorous validation in more complex systems or future clinical studies.

Conclusion

In summary, our findings identify BSG-D as a novel and promising candidate for treatment T2DM. This natural alkaloid markedly improves hyperglycemia, dyslipidemia, and insulin resistance through the synergistic activation of PI3K/AKT and AMPK signaling pathways. These findings not only underscore the therapeutic potential of BSG-D but also highlight a multi-target mechanism that may offer advantages over single-pathway agents.

Funding

The project was sponsored by National Nature Science Foundation of China (82204795), Shandong Provincial Natural Science Foundation (ZR2020QH329).

Declaration of competing interest

The authors declare that they have no known competing financial interests or personal relationships that could have appeared to influence the work reported in this paper.

Acknowledgement

We are grateful to Shandong Co-Innovation Center of Classic TCM Formula for providing facility to conduct this work. We also thank members of the Shandong Co-Innovation Center of Classic TCM Formula, for their support and encouragement.

Conflict of Interest

The authors declare no competing financial interests.

Author contributions

Hedi Wang: Performed part of the experiments;Data curation; Data visualisation formal analysis; Visualization; Writ-ing-original draft. Qiang Chen: Performed part of the experiments;Data collection. Qianhui Ning: Assisted with animal experiments.Yanting Lu,Zhiwei Wang: Conceptualisation; Writing- Re-viewing. All authors have read and approved the manuscript

Declarations

Ethics approval and consent to participate

All animal experiments and procedures in this study were performed in compliance with the regulations on the management and welfare of laboratory animals, and were approved by the Animal Ethics Committee of Shandong University of Traditional Chinese Medicine (Approval No. SDUTCM20210301018).

Consent for publication

Not Applicable.

Availability of data and materials

Not Applicable.

Competing interests

The authors have declared that no competing interests exist.

Funding

This work was supported by the National Natural Science Foundation of China(82204795) and Natural Science Foundation of Shandong Province(ZR2020QH329)

Authors' contributions

Conceptualization: Hedi Wang, Zhiwei Wang, Yanting Lu; Methodology: Hedi Wang, Qiang Chen; Software: Hedi Wang, Qiang Chen; Validation: Qianhui Ning, Zhiwei Wang; Formal analysis: Hedi Wang, Qiang Chen; Investigation: Hedi Wang, Yanting Lu; Resources:Qianhui Ning; Data curation: Hedi Wang,Qiang Chen; Writing – original draft: Hedi Wang; Writing – review & editing: Zhiwei Wang, Yanting Lu; Visualization: Hedi Wang, Yanting Lu; Supervision: Zhiwei Wang, Yanting Lu; Project administration: Yanting Lu; Funding acquisition:Zhiwei Wang, Yanting Lu.

Acknowledgements

This work was supported by the National Natural Science Foundation of China(82204795) and Natural Science Foundation of Shandong Province(ZR2020QH329)

Reference

1. Zheng Y, Ley SH, Hu FB. Global aetiology and epidemiology of type 2 diabetes mellitus and its complications. Nat Rev Endocrinol. 2018;14(2):88-98. doi:10.1038/nrendo.2017.151

2. Bjornstad P, Chao LC, Cree-Green M, et al. Youth-onset type 2 diabetes mellitus: an urgent challenge. Nat Rev Nephrol. 2023;19(3):168-184. doi:10.1038/s41581-022-00645-1

3. Ahmad E, Lim S, Lamptey R, Webb DR, Davies MJ. Type 2 diabetes. Lancet. 2022;400(10365):1803-1820. doi:10.1016/S0140-6736(22)01655-5

4. GBD 2021 Diabetes Collaborators. Global, regional, and national burden of diabetes from 1990 to 2021, with projections of prevalence to 2050: a systematic analysis for the Global Burden of Disease Study 2021. Lancet. 2023;402(10397):203-234. doi:10.1016/S0140-6736(23)01301-6

5. Giugliano D, Standl E, Vilsbøll T, et al. Is the current therapeutic armamentarium in diabetes enough to control the epidemic and its consequences? What are the current shortcomings?. Acta Diabetol. 2009;46(3):173-181. doi:10.1007/s00592-009-0134-3

6. Ni HX, Cao LH, Gong XX, Zang ZY, Chang H. Traditional Chinese medicine for treatment of type 2 diabetes mellitus: Clinical evidence and pharmacological mechanisms. J Integr Med. 2025;23(6):605-622. doi:10.1016/j.joim.2025.08.006

7. S.-y. Li, C.-t. Yang, X.-l. Zeng, Z.-y. Jiang, K. Tian, J.-x. Sun, X.-Z. Huang, Study on the chemical constituents in the stems of Bousigonia mekongensis, J. Yunnan Univ. Nat. (Nat. Sci. Ed.) 23 (2014) 235–238.

8. Shi K, Li X, Chen R, et al. BSG-D from Bousigonia mekongensis inhibits bladder cancer growth and overcomes cisplatin resistance. Sci Rep. 2025;15(1):16254. Published 2025 May 9. doi:10.1038/s41598-025-96892-w

9. Huo ZQ, Zhao Q, Zhu WT, Hao XJ, Zhang Y. Bousmekines A-E, New Alkaloids from Two Bousigonia Species: B.angustifolia and B. mekongensis. Nat Prod Bioprospect. 2021;11(2):207-213. doi:10.1007/s13659-020-00278-6

10. Zhang Y, Goto M, Oda A, et al. Antiproliferative Aspidosperma-Type Monoterpenoid Indole Alkaloids from Bousigonia mekongensis Inhibit Tubulin Polymerization. Molecules. 2019;24(7):1256. Published 2019 Mar 31. doi:10.3390/molecules24071256

11. Fu YH, Li SL, Li SF, et al. Cytotoxic eburnamine-aspidospermine type bisindole alkaloids from Bousigonia mekongensis. Fitoterapia. 2014;98:45-52. doi:10.1016/j.fitote.2014.07.008

12. Wang ZW, Wang YL, Zhang JP, Wei QH, Wang XJ. Monoterpene indole alkaloids from the roots of Bousigonia mekongensis and their anti-diabetic nephropathy activity. Fitoterapia. 2021;153:104964. doi:10.1016/j.fitote.2021.104964

13. Regina I, Tong F. Overview of insulin: more than a hormone for controlling glucose level. Biomed Eng Commun. 2025;4(2):10. doi:10.53388/BMEC2025010

14. Cao R, Tian H, Zhang Y, et al. Signaling pathways and intervention for therapy of type 2 diabetes mellitus. MedComm (2020). 2023;4(3):e283. Published 2023 Jun 7. doi:10.1002/mco2.283

15. Feng Y, Ren Y, Zhang X, et al. Metabolites of traditional Chinese medicine targeting PI3K/AKT signaling pathway for hypoglycemic effect in type 2 diabetes. Front Pharmacol. 2024;15:1373711. Published 2024 May 10. doi:10.3389/fphar.2024.1373711

16. Chen J,Liu B,Yang X, et al. AMPK/SIRT1/PGC-1α Signaling Pathway: Molecular Mechanisms and Targeted Strategies From Energy Homeostasis Regulation to Disease Therapy. CNS Neurosci Ther. 2025;31 (11):e70657. doi:10.1111/cns.70657

17. Cui J, Li H, Zhang T, et al. Research progress on the mechanism of curcumin anti-oxidative stress based on signaling pathway. Front Pharmacol. 2025;16:1548073. Published 2025 Apr 7. doi:10.3389/fphar.2025.1548073

18. Cui X, Chen Z, Xu L, Wu C, Zhou C. Metabolic profile alterations in juvenile rats with bladder overactivity induced by short-term high-fructose intake. PeerJ. 2025;13:e20186. Published 2025 Oct 13. doi:10.7717/peerj.20186

19. Prakash T, Ramachandra NB. Prioritizing Candidate Genes for Type 2 Diabetes Mellitus using Integrated Network and Pathway Analysis. Avicenna J Med Biotechnol. 2022;14(3):239-246. doi:10.18502/ajmb.v14i3.9831

20. Mazibuko-Mbeje SE, Dludla PV, Roux C, et al. Aspalathin-Enriched Green Rooibos Extract Reduces Hepatic Insulin Resistance by Modulating PI3K/AKT and AMPK Pathways. Int J Mol Sci. 2019;20(3):633. Published 2019 Feb 1. doi:10.3390/ijms20030633

21. White MF. Insulin signaling in health and disease. Science. 2003;302(5651):1710-1711. doi:10.1126/science.1092952

22. Uehara K, Lee WD, Stefkovich M, et al. mTORC1 controls murine postprandial hepatic glycogen synthesis via Ppp1r3b. J Clin Invest. 2024;134(7):e173782. Published 2024 Jan 30. doi:10.1172/JCI173782

23. Liu TY, Shi CX, Gao R, et al. Irisin inhibits hepatic gluconeogenesis and increases glycogen synthesis via the PI3K/Akt pathway in type 2 diabetic mice and hepatocytes. Clin Sci (Lond). 2015;129(10):839-850. doi:10.1042/CS20150009

24. Hajiaghaalipour F, Khalilpourfarshbafi M, Arya A. Modulation of glucose transporter protein by dietary flavonoids in type 2 diabetes mellitus. Int J Biol Sci. 2015;11(5):508-524. Published 2015 Mar 19. doi:10.7150/ijbs.11241

25. Serum- and glucocorticoid-induced kinase drives hepatic insulin resistance by directly inhibiting AMP-activated protein kinase

26. Gong P,Wang X,Yang W, et al. Hypoglycemic activity of enzymatically extracted Eucommia ulmoides polysaccharide (EUL-w1) on IR-HepG2 cell via the AMPK/PI3K/Akt signaling pathway. Int J Biol Macromol. 2024;283 (Pt 1):137596. doi:10.1016/j.ijbiomac.2024.137596

27. Zhao Y,Hu X,Liu Y, et al. ROS signaling under metabolic stress: cross-talk between AMPK and AKT pathway. Mol Cancer. 2017;16 (1):79. doi:10.1186/s12943-017-0648-1

28. Zheng T, Yang X, Wu D, et al. Salidroside ameliorates insulin resistance through activation of a mitochondria-associated AMPK/PI3K/Akt/GSK3β pathway. Br J Pharmacol. 2015;172(13):3284-3301. doi:10.1111/bph.13120

29. Wang Y, Liu G, Liu X, et al. Serpentine Enhances Insulin Regulation of Blood Glucose through Insulin Receptor Signaling Pathway. Pharmaceuticals (Basel). 2022;16(1):16. Published 2022 Dec 22. doi:10.3390/ph16010016

30. Yao XG, Chen F, Li P, et al. Natural product vindoline stimulates insulin secretion and efficiently ameliorates glucose homeostasis in diabetic murine models. J Ethnopharmacol. 2013;150(1):285-297. doi:10.1016/j.jep.2013.08.043

31. Oguntibeju OO, Aboua Y, Goboza M. Vindoline-A Natural Product from Catharanthus Roseus Reduces Hyperlipidemia and Renal Pathophysiology in

Experimental Type 2 Diabetes. Biomedicines. 2019;7(3):59. Published 2019 Aug 13. doi:10.3390/biomedicines7030059

32. Shijina BN, Radhika A, Sherin S, Biju PG. Vindoline Exhibits Anti-Diabetic Potential in Insulin-Resistant 3T3-L1 Adipocytes and L6 Skeletal Myoblasts. Nutrients. 2023;15(13):2865. Published 2023 Jun 24. doi:10.3390/nu15132865

33. Shittu, H., Gray, A., Furman, B., & Young, L. (2010). Glucose uptake stimulatory effect of akuammicine from Picralima nitida (Apocynaceae). Phytochemistry Letters, 3(1), 53-55.

34. Tiong SH, Looi CY, Hazni H, et al. Antidiabetic and antioxidant properties of alkaloids from Catharanthus roseus (L.) G. Don. Molecules. 2013;18(8):9770-9784. Published 2013 Aug 15. doi:10.3390/molecules18089770

Supplementary Files

This is a list of supplementary files associated with this preprint. Click to download.

- S1.jpg
- Blotsimages.pdf